

MODELING OF HEXAGONAL BORON NITRIDE FILLED BISMALEMIDE
POLYMER COMPOSITES FOR THERMAL PROPERTIES
FOR ELECTRONIC PACKAGING

Md Salah Uddin

Thesis Prepared for the Degree of
MASTER OF SCIENCE

UNIVERSITY OF NORTH TEXAS

December 2016

APPROVED:

Nandika D'Souza, Major Advisor
Tae-Youl Choi, Co-Major Advisor
Zhenhai Xia, Committee Member
Kuruvilla John, Chair of the Department of
Mechanical and Energy Engineering
Costas Tsatsoulis, Dean of College of
Engineering
Victor Prybutok, Vice Provost of the
Toulouse Graduate School

ProQuest Number: 10586918

All rights reserved

INFORMATION TO ALL USERS

The quality of this reproduction is dependent upon the quality of the copy submitted.

In the unlikely event that the author did not send a complete manuscript and there are missing pages, these will be noted. Also, if material had to be removed, a note will indicate the deletion.



ProQuest 10586918

Published by ProQuest LLC (2017). Copyright of the Dissertation is held by the Author.

All rights reserved.

This work is protected against unauthorized copying under Title 17, United States Code
Microform Edition © ProQuest LLC.

ProQuest LLC.
789 East Eisenhower Parkway
P.O. Box 1346
Ann Arbor, MI 48106 – 1346

Uddin, Md Salah, *Modeling of Hexagonal Boron Nitride Filled Bismaleimide Polymer Composites for Thermal Properties for Electronic Packaging*. Master of Science (Mechanical and Energy Engineering), December 2016, 39 pp, 3 tables, 24 figures, chapter references.

Miniaturization of electronic devices and high power densities require faster heat transfer to avoid the thermal failure. Die-attach polymer adhesives are used to bond chips in electronic packaging. These adhesives should have high mechanical, thermal, dielectric, and moisture resistant properties. As polymers are insulators, thermally conductive particles are mixed into them to enhance the thermal flow. The need to concurrently maintain electrically insulative characteristics led to use of Boron Nitride as the filler. This thesis focuses on the characterization of polymer composites for thermal and electrical properties with experimental and computational tools. Platelet geometry of hexagonal boron nitride offers highly anisotropic properties. Therefore, their alignment and degree of orientation offers tunable properties in polymer composites for thermal, electrical, and mechanical properties. This thesis intends to model the anisotropic behavior of thermal properties using finite element and molecular dynamics simulations and compare to measurements done previously.

Copyright 2016

by

Md Salah Uddin

ACKNOWLEDGEMENTS

My immense gratitude to my advisor Dr. Nandika D'Souza for supporting my Master's thesis. I am highly indebted for her guidance, inspiration, concepts and support for this study.

I would like to appreciate Dr. Tae-Youl Choi for being my co-major advisor and the valuable discussion. I appreciate Dr. Zhenhai Xia for being my committee member and helping me with learning molecular simulations.

I acknowledge Semiconductor Research Corporation (SRC) through the grant GRC TASK 2389.001 and Advanced Materials & Manufacturing Processes Institute (AMMPI) at UNT for supporting this thesis.

I thank my friends and colleagues Andres Garcia, Hussain R. Rizvi, Nathan Warner, Zachary Hoyt, Hyeonu Heo, Amaal Al-Shenawa, Yuvaraj Chitela, and Changlei Xia for their help up to this point.

I am grateful to my parents who has always prayed for my success and appreciative to my wife for standing beside me.

The following tables and figures are reproduced with permission from the Semiconductor Research Corporation (SRC) Annual Review Presentation, 2016, Boron Nitride Thermally Conductive High Temperature High Dielectric Strength Interface Materials, Publication ID: P087924, June 7-9:

- Table 1-1
- Figure 1-2, Figures 2-1 to 2-10
- Figures 2-12 to 2-14
- Figures 3-1 to 3-6
- Figure 4-1 (c)

TABLE OF CONTENTS

	Page
ACKNOWLEDGEMENTS	iii
LIST OF TABLES	vi
LIST OF FIGURES	vii
CHAPTER 1 INTRODUCTION	1
1.1 Background	1
1.2 References	3
CHAPTER 2 FINITE ELEMENT ANALYSIS OF THERMAL CONDUCTIVITY	5
2.1 Introduction	5
2.2 Experimental	7
2.2.1 Sample Preparation	7
2.2.2 Hot Disk Thermal	7
2.3 FEA-1	9
2.3.1 Microstructure Modeling	9
2.3.2 Materials Properties	11
2.3.3 Skeleton, Meshing, and Refinement	11
2.3.4 Fields, Equation, and Boundary Condition	13
2.4 Results and Analysis	13
2.4.1 Orientation Effect	14
2.4.2 Diameter Effect	15
2.4.3 Effect of Particle Interconnected Network	16
2.5 Comparison with Experiments	17
2.6 FEA-2	18
2.7 Conclusions	21
2.8 References	22
CHAPTER 3 MOLECULAR DYNAMICS SIMULATIONS FOR THERMAL CONDUCTIVITY	25
3.1 Introduction	25
3.2 Methodology	26

3.2.1	Constructing Molecular Model	26
3.2.2	Reverse Non-Equilibrium Molecular Dynamics (RNEMD) Simulation..	29
3.3	Results	31
3.4	Conclusions	34
3.5	References	35
CHAPTER 4 CONCLUSIONS		37
4.1	References	39

LIST OF TABLES

	Page
Table 1-1: Comparison of thermal and electrical properties of different nanoparticles	1
Table 2-1: Measured thermal conductivity of BMI and BN-BMI composites in experiments	9
Table 2-2: Predicted thermal conductivity of BN-BMI composites in FEA-1	15

LIST OF FIGURES

	Page
Figure 1-1: Aircraft radomes protecting the radar antenna.....	2
Figure 1-2: Anisotropic thermal properties of CNT (top) and BN (bottom) fillers [3-4].....	3
Figure 2-1: Hot disk sensor working as both a heat source and a sensing element.....	8
Figure 2-2: Measured thermal conductivity of BN-BMI composites at different wt% of BN platelets.	9
Figure 2-3: Three different orientations and boundary conditions of steady state heat transfer analysis of boron nitride platelet filled bismaleimide composite: (a) case-1 (longitudinal), (b) case-2 (perpendicular), and (c) case-1 (angled).....	10
Figure 2-4: Materials properties for the thermal model [5]	11
Figure 2-5: Homogeneity index of the element [12]	12
Figure 2-6: A portion of a meshed sample.....	13
Figure 2-7: Thermal conductivity versus volume fraction at three different orientation calculated using OOF2 software.	14
Figure 2-8: Temperature (left) and heat flux (right) contour plot of three different orientations: (a) case-1 (longitudinal), (b) case-2 (perpendicular), and (c) case-1 (angled).....	15
Figure 2-9: Thermal conductivity vs. diameter of the platelet at a fixed aspect ratio and weight %	16
Figure 2-10: The effect of thermal conductivity of particle interconnection (80% BN by wt.)..	17
Figure 2-11: Comparison of simulation thermal conductivity with experimental values.	18
Figure 2-12: SEM images of BN platelet filled BMI: 20% (left) and 80% (right) weight fraction of BN [18].	19
Figure 2-13: Polished SEM image of 80% BN platelets, a portion of the meshed structure and temperature profile.....	19
Figure 2-14: Comparison between the predicted and experimental thermal conductivity based on SEM images of 20% and 80%	21
Figure 3-1: Molecular structure of cross-linked BMI (monomer is in the inset).....	28
Figure 3-2: Three different orientations of the BN platelets of BN-BMI composite at 57% weight percentage of BN.	29

Figure 3-3: Contour plot of temperature gradient of the simulation box (left), temperature gradient along Z-direction (right)	31
Figure 3-4: Thermal conductivity at three different orientations at 39% weight fraction of BN platelets	32
Figure 3-5: Thermal conductivity at three different orientations at 56% weight fraction of BN platelets	33
Figure 3-6: Thermal conductivity at three different orientations at 80% weight fraction of BN platelets	33
Figure 3-7: Comparison of predicted results from molecular dynamics simulations with the experimental measurements.....	34
Figure 4-1: (a) Comparison of FEA with experiments, (b) comparison of MD simulations with experiment, and (c) comparison of FEA, MD simulations, and experiment.	38

CHAPTER 1

INTRODUCTION

1.1 Background

Die attached adhesives have to exhibit excellent dielectric properties, heat-resistant properties, mechanical properties, and feasible processing characteristics. Epoxies and polyimide (PI) have been used for low relative permittivity and loss [1-2]. But, they have bad hot-wet properties (readily absorb atmospheric moisture even in hot, dry climates), high dielectric loss, high viscosity. Over the last two decade, bismaleimide (BMI) has been used in both the electronic and aerospace industries, because of their excellent elevated temperature and dielectric properties, low moisture absorption, constant electrical properties over a wide range of temperatures and good flammability characteristics [2]. Therefore, BMI is utilized as a resin of the polymer composites. In order to maximize the heat transfer and dielectric strength, we intend to reinforce the resin with nanoparticles. Several fillers have also been investigated, where silica, silver, and carbon nanotube (CNT) have limitations either in thermal or electrical properties. One the other hand, boron nitride (BN) has been estimated as the superior to others in terms of both thermal conductivity and dielectric strength as mentioned in the Table 1-1.

Table 1-1: Comparison of thermal and electrical properties of different nanoparticles

Silica	Dielectric strength↑	Thermal conductivity↓
Silver	Thermal conductivity↑	Dielectric strength↓
CNT	Thermal conductivity↑	Electrical conductivity↑
BN	Thermal conductivity↑	Dielectric strength↑

Along with the electronic industries, high dielectric and thermal properties are also a matter of interest in aerospace industries [1]. Polymers and their composites are used as the main structural component or coatings in ground, marine, and aircraft radomes applications, which protect the

radar antenna as shown in Figure 1-1. Signal must go through the radomes without impedance for a better performance of the radar, which requires excellent dielectric properties. High heat resistant is obviously needed for aircraft coating.



Figure 1-1: Aircraft radomes protecting the radar antenna.

Boron nitride, similar to CNT, is highly anisotropic [3-4]. In order to align the BN platelets in the composites, magnetically responsive BN platelets are produced by the surface modification of iron oxide, which are then directed by an external magnetic field. It has been reported that alignment of CNT and BN fillers would maximize the in-plane properties as shown in Figure 1-2 [3, 4]. Therefore, this thesis mainly focuses on modeling techniques for anisotropic properties of BN-reinforced BMI crosslinked polymer composites. Validation is performed with experimental results.

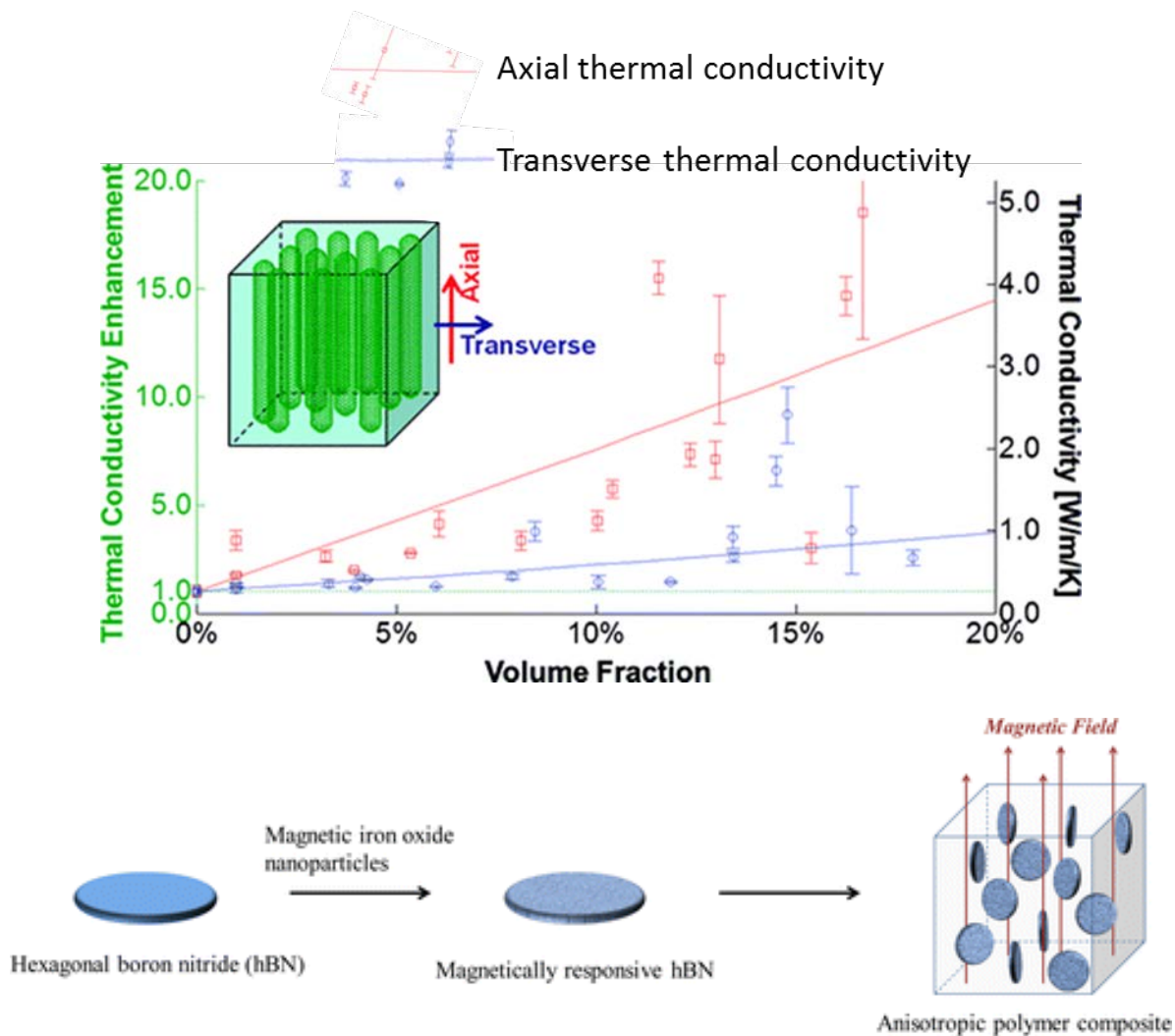


Figure 1-2: Anisotropic thermal properties of CNT (top) and BN (bottom) fillers [3-4].

1.2 References

1. García, C., Fittipaldi, M., & Grace, L. R. (2015). Epoxy/montmorillonite nanocomposites for improving aircraft radome longevity. *Journal of Applied Polymer Science*, 132(43).
2. Liang, G., Zhang, Z., Yang, J., & Wang, X. (2007). BMI based composites with low dielectric loss. *Polymer Bulletin*, 59(2), 269-278.
3. Marconnet, A. M., Yamamoto, N., Panzer, M. A., Wardle, B. L., & Goodson, K. E. (2011). Thermal conduction in aligned carbon nanotube-polymer nanocomposites with high packing density. *ACS nano*, 5(6), 4818-4825.

4. Lin, Z., Liu, Y., Raghavan, S., Moon, K. S., Sitaraman, S. K., & Wong, C. P. (2013). Magnetic alignment of hexagonal boron nitride platelets in polymer matrix: toward high performance anisotropic polymer composites for electronic encapsulation. *ACS applied materials & interfaces*, 5(15), 7633-7640.

CHAPTER 2

FINITE ELEMENT ANALYSIS OF THERMAL CONDUCTIVITY

2.1 Introduction

Development of composite materials for thermal management in electronic packaging has always been challenging in terms of high thermal conductivity, low coefficient of thermal expansion, high strength to weight ratio, low cost, and fabrication processes [1]. Carbon nanotube, graphene/graphite, silica, alumina are used to reinforce the polymer for the enhancement of thermal conductivity whereas carbon based filler was found to be very effective [2-4]. But as carbon based filler also increases the electrical conductivity, boron nitride based polymer composite is now attracting the researchers for high-conductive, high-dielectric materials for electronics [5-11]. Anisotropic thermal properties of BN platelets has been discussed by several authors [5-7]. Therefore, alignment of the fillers in polymer will maximize the thermal transport.

Finite element models for particle reinforced composite have been developed in order to predict thermal conductivity using object oriented finite element analysis (OOF2) tool [12-17]. This FE analysis helps to understand the behavior of particle reinforced composites and overcome the limitation of the rule of mixture, which overestimates the properties for these kinds of composites. Because, the effective properties of the composites are proportionate to the properties of resins and reinforcing elements to their volume fraction according to the rule of mixture, which does not consider the dispersion and anisotropic properties of the reinforcing elements [14]. Bakshi et al showed that the nanocluster of carbon nanotube has less thermal conductivity than an individual one which reduces the overall performance of the composite significantly [14]. But the effect of bulk properties of the composite due to the anisotropy raised from the particle such as hexagonal boron nitride is yet to investigate.

In order to understand the anisotropic thermal conductivity in bulk material of hexagonal boron nitride (BN) platelets filled bismaleimide composite, we perform finite element analysis. Anisotropic materials property of BN platelets is used whereas the bismaleimide resin is considered as isotropic in this study. OOF2 is used to simulate the steady state thermal behavior of the composite to determine its effective thermal conductivity at different weight fractions in different orientations. The FEA analysis is performed on two types of microstructures: modeled microstructures and scanning electron microscope (SEM) microstructures. Two-dimensional microstructures of the composite are modeled with three different orientations of the platelets: longitudinal, perpendicular, and angled to the direction of the bulk sample to measure thermal conductivity for FEA-1. The second FE Analysis (FEA-2) deals with real distribution of the platelets obtained from SEM images of the composites with two different weight percentages (20% and 80%) of platelets. The microstructures are meshed with very fine triangular geometry with homogeneity index as 0.998. A temperature gradient is imposed by setting the temperature at left side as 100°C and the right side as 0°C whereas two other sides (top and bottom) are set as adiabatic ($Q = 0$) boundary condition to impose one dimensional heat flow. Angle *et al.* reported temperature dependent thermal conductivities, which showed that OOF2 is not very sensitive to the temperature values at the two ends and requires only a reasonable temperature gradient at the boundaries [16]. Conventional steady state heat flux equation is solved to find the flux rate required to maintain that gradient. Longitudinal and perpendicular orientation of the platelets define the upper and lower limit of the thermal conductivity and the angled platelets fall within the limit which shows the model as performing. For validation purposes, simulation results are compared with the results obtained from experiments.

2.2 Experimental

2.2.1 Sample Preparation

The preparation of the composite in all filler loadings begins with the preparation of the bismaleimide (BMI) provided by Cytec Materials (CYCOM 5250-4 RTM Resin System, a three part liquefying BMI). The BMI is refined into an ultrafine powder using a cryogenic mill for the purpose of evenly dispersing into hexagonal boron nitride. As BMI starts crosslinking at room temperature, BMI and BN are mixed in a cryogenic environment with liquid nitrogen and stirred vigorously. During the mixing and stirring process continuous evaporation of liquid nitrogen prohibits any external moisture to be absorbed by the material in its uncured state. Liquid nitrogen both dries the BMI and allows any filler loading to be introduced evenly into the polymer matrix. Afterward, the mix was immediately transferred to the heated platter of the compression molding and care has been taken so that no moisture is absorbed. The particulate reinforcement, and thermal modifier of the experiment is hexagonal boron nitride (hBN), obtained from Momentive Performance Materials in grades PT110 (50 μ m average platelet size) and Lower Friction supplied the 0.07 μ m platelets.

2.2.2 Hot Disk Thermal

The thermal conductivities of the samples were measured using a Hot Disk TPS 1500 Thermal Conductivity System. A thin-film heating element (“Hot Disk Sensor”) is placed between two identical samples and enclosed inside an adiabatic chamber as shown in Figure 2-1. The thin film heating element acts as both a heater and a resistance temperature detector. Power is applied at a fixed rate during testing and the machine records temperature increase with time. With a known sample geometry, temperature increment is used to determine the bulk thermal conductivity

and volumetric specific heat of the sample. Volumetric specific heat and sample geometry are then updated within the testing system and measurements of thermal conductivity are carried out. All thermal conductivity values are obtained at room temperature. The reported values are corrected for porosity, which effect is considered as negligible. The difference between theoretical and experimental composite density is measured and porosity is taken to be the missing fraction of the material. The measured effective thermal conductivity of the composite is scaled by the porosity percentage then added to the original value to represent corrected thermal conductivity. Measured thermal conductivities of pure BMI and the composites at different weight % of BN are reported in Figure 2-2 and Table 2-1, which are taken from previous study [18]. It is observed that the thermal conductivity increases sharply at higher concentrations due to the formation of particle inter-connections specifically at 70% and 80% loading fractions of BN by wt.%. In spite of having such higher thermal conductivities at higher concentrations, higher filler loadings are normally avoided because of having less binding material i.e., the polymer resin, life and reliability of the composites are compromised. Additionally, as the polymer composite is targeted to be used as adhesives, its adhesive strength may also be hampered.

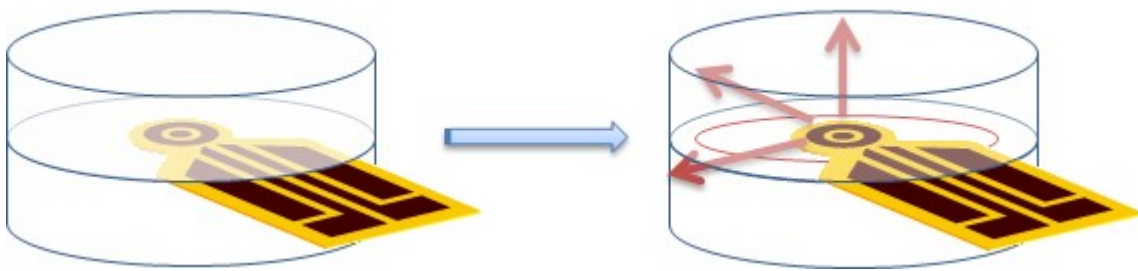


Figure 2-1: Hot disk sensor working as both a heat source and a sensing element.

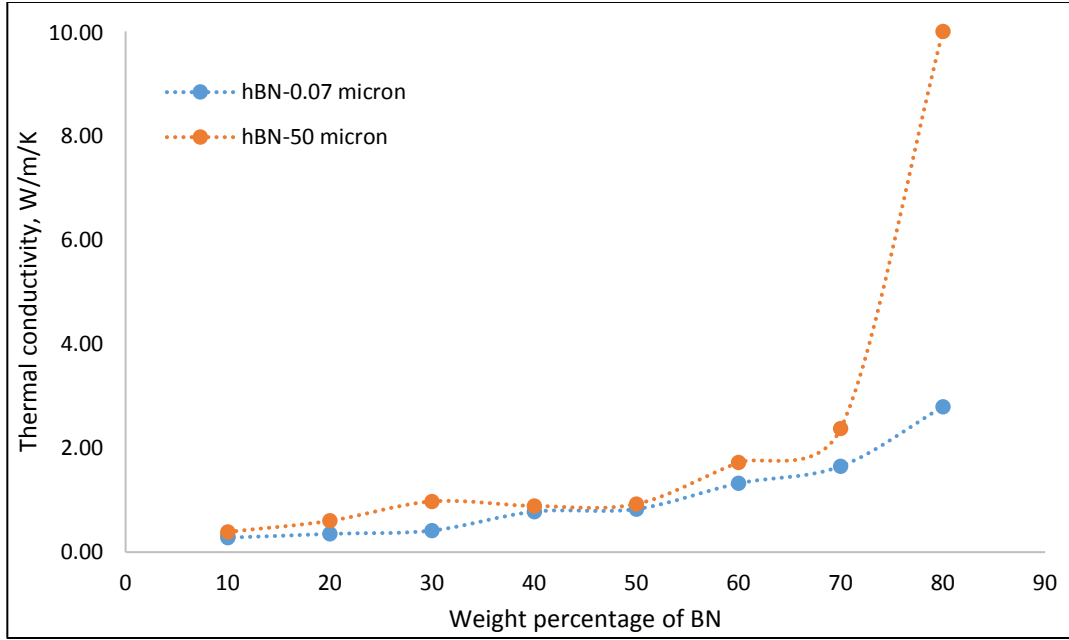


Figure 2-2: Measured thermal conductivity of BN-BMI composites at different wt% of BN platelets.

Table 2-1: Measured thermal conductivity of BMI and BN-BMI composites in experiments

Sample	Experimental Thermal Conductivity ($W/m/K$)	
	0.07 micron BN	50 micron BN
Pure BMI		0.19
10% BN	0.32	0.39
20% BN	0.352	0.60
30% BN	0.42	0.98
40% BN	0.78	0.89
50% BN	0.83	0.98
60% BN	1.324	1.73
70% BN	1.65	2.38
80% BN	2.8	10.03

2.3 FEA-1

2.3.1 Microstructure Modeling

OOF works on image file of microstructure. Binary image files of the composite is prepared for three different orientations with different volume fractions of the filler. Figure 2-3 shows the orientation and microstructure of the two-dimensional models. These two-dimensional

microstructure domains are $350\mu\text{m} \times 350\mu\text{m}$. In order to make sure the adiabatic boundary condition and one-dimensional flow, the vertical dimension should be large enough compared to the direction of heat flow in an experiment. However, in this simulation, the system is forced to be a one-dimensional heat flow regardless the dimension of the sample by assigning no temperature gradient in the vertical direction.

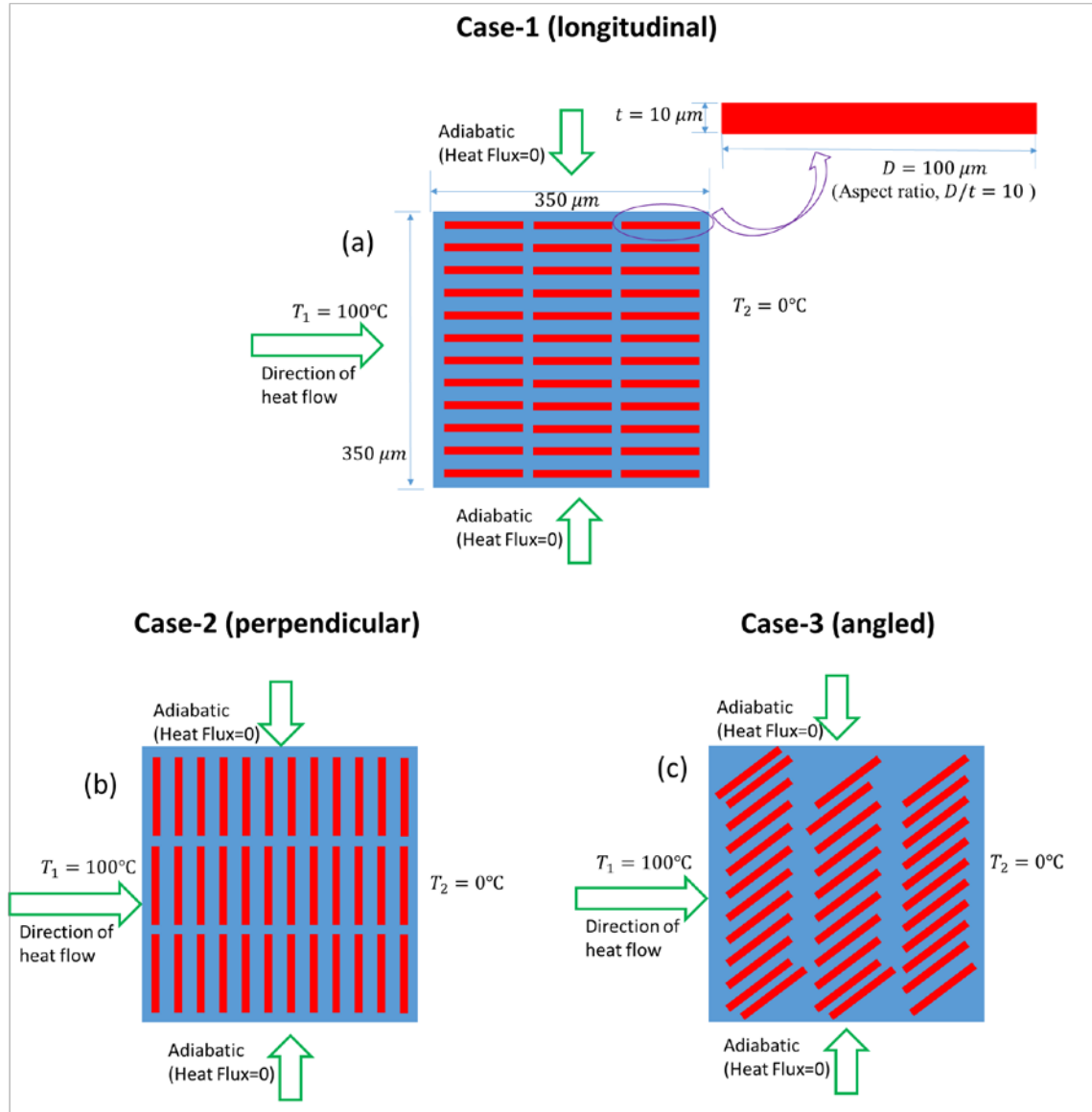


Figure 2-3: Three different orientations and boundary conditions of steady state heat transfer analysis of boron nitride platelet filled bismaleimide composite: (a) case-1 (longitudinal), (b) case-2 (perpendicular), and (c) case-1 (angled).

Perfect alignment and homogeneous distributions of the platelets are considered for simplicity. Samples are prepared with different volume fractions of the filler with a range of 17-70% (24%-80% by wt.). Three different orientations for 30% volume fraction of BN is with the thermal boundary condition is depicted in Figure 2-3. In order to define distinct phases of platelets and resin, pixel selection with color tool is used.

2.3.2 Materials Properties

Anisotropic thermal conductivity of BN platelets is used whereas isotropic condition is assumed for the bismaleimide resin as shown in Figure 2-4. Anisotropic orthorhombic materials properties for the filler is assigned in OOF2 whereas direction-3 will automatically be neglected for being a two-dimensional problem.

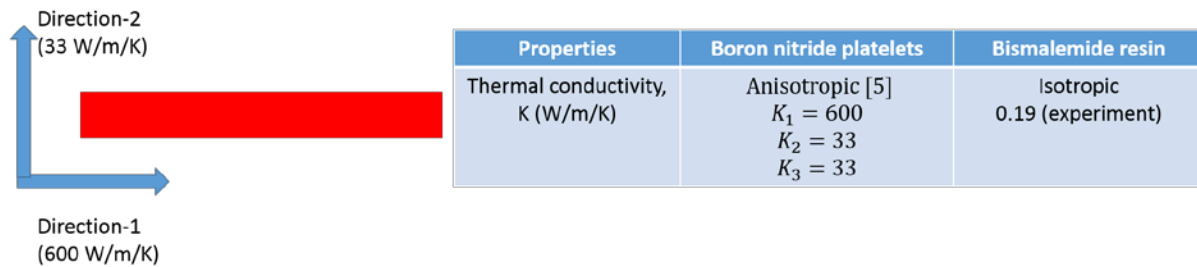


Figure 2-4: Materials properties for the thermal model [5]

2.3.3 Skeleton, Meshing, and Refinement

Skeleton is created on the microstructure prior to mesh where the skeleton defines only the geometry of the mesh with no other information of shape functions or any other equations. Triangular elements with non-periodicity of the mesh are created where initial homogeneity index (HI) is 0.94. For a better solution, HI should be as maximum as possible. This index defines how well the skeleton geometry matches with distinct phases of the composite selected by pixel

selection by color where each phase has been assigned with different material properties [12]. The ratio of the area of the dominant category to the area of the element as a whole is defined as homogeneity. The homogeneity of a completely homogeneous element is 1.0. Figure 2-5 shows three different materials with different colors where top right element has homogeneity as 1.0, middle one as 0.5 and the leftmost has 0.3 [12].

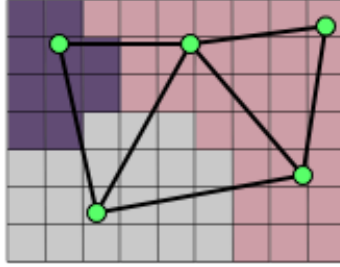


Figure 2-5: Homogeneity index of the element [12]

Effective energy functional (E) of the mesh is used to control the homogeneity with different operations such as anneal, swap edges, smooth, and refine. This functional assigns a number between 0 and 1 to each element which plays a role of the energy in the statistical mechanical simulation process for various operations to increase the homogeneity of the elements. The functional has to compromise between two contributions: homogeneity and shape using α as the following equation:

$$E = \alpha E_{homog.} + (1 - \alpha) E_{shape} \quad (1-1)$$

After a series of operations consisting of annealing, swapping edges, smoothing, and refining the final homogeneity index is 0.998 with 14641 nodes and 28800 elements which reaches the convergence of mesh dependence. The HI as 0.998 means 99.8% meshes are within the region of the same phase and do not share with different phases i.e. platelets and resin. Finally the FE mesh is performed on this skeleton. Figure 2-6 shows a portion of a meshed structure.

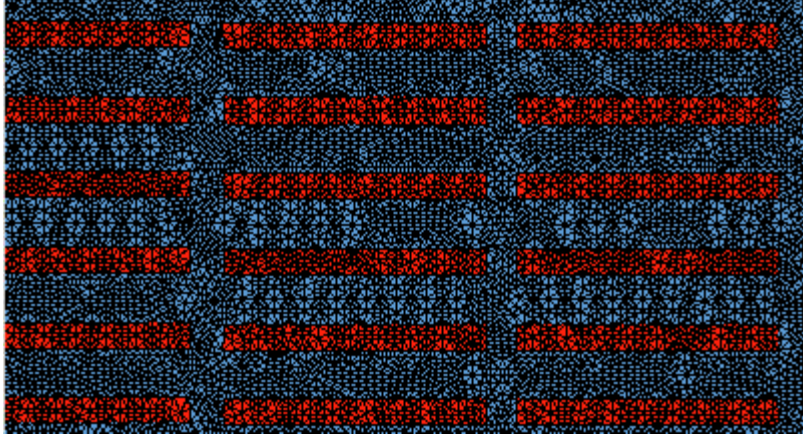


Figure 2-6: A portion of a meshed sample

2.3.4 Fields, Equation, and Boundary Condition

In order to solve the developed model, a similar approach by Bakshi *et al.* is followed [14]. The conventional heat flux and heat equation are solved using the conjugate gradient (CG) method [12]. The boundary conditions for different orientations are depicted in Figure 2-3. The left and right sides are assigned with constant temperatures as 100°C and 0°C respectively. Top and bottom boundaries are made adiabatic to make the heat flow one dimensional. OOF2 solver reaches the convergence to calculate heat flux for the imposed temperature gradient using CG method with a relative error of 1×10^{-13} .

2.4 Results and Analysis

Fourier heat conduction equation is used to determine the effective thermal conductivity from the integrated heat flux at the right boundary and temperature gradient as the following equation:

$$\langle q \rangle = -k_{eff} \cdot \langle \nabla T \rangle \quad (1-2)$$

where, k_{eff} is the effective thermal conductivity of the composite, $\langle q \rangle$ is the normalized integrated heat flux at the right boundary, and $\langle \nabla T \rangle$ is temperature gradient.

2.4.1 Orientation Effect

Effective thermal conductivity is measured for different wt% in three different orientations as mentioned in Figure 2-3. The effective thermal conductivities are reported in Figure 2-7 which shows that the longitudinal and perpendicular directions set the upper and lower limit, where the angled platelet reinforced composites fall in between the limits. Contour plots of temperature (left) and heat flux (right) for three different orientations are shown in Figure 2-8. The results from FEA-1 with different loading fraction at three different orientations are reported in Table 2-2.

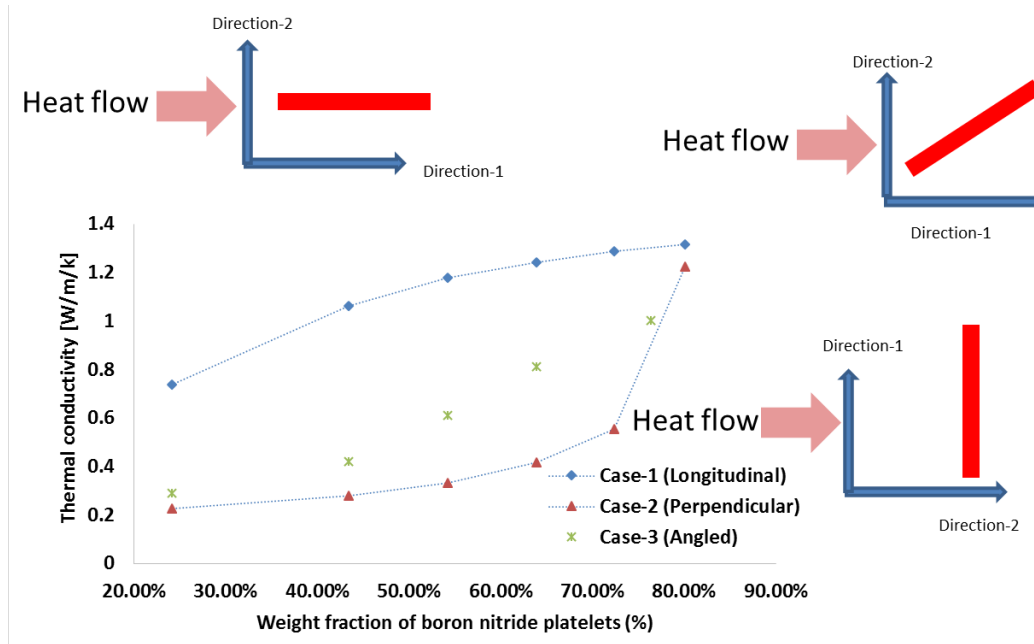


Figure 2-7: Thermal conductivity versus volume fraction at three different orientation calculated using OOF2 software.

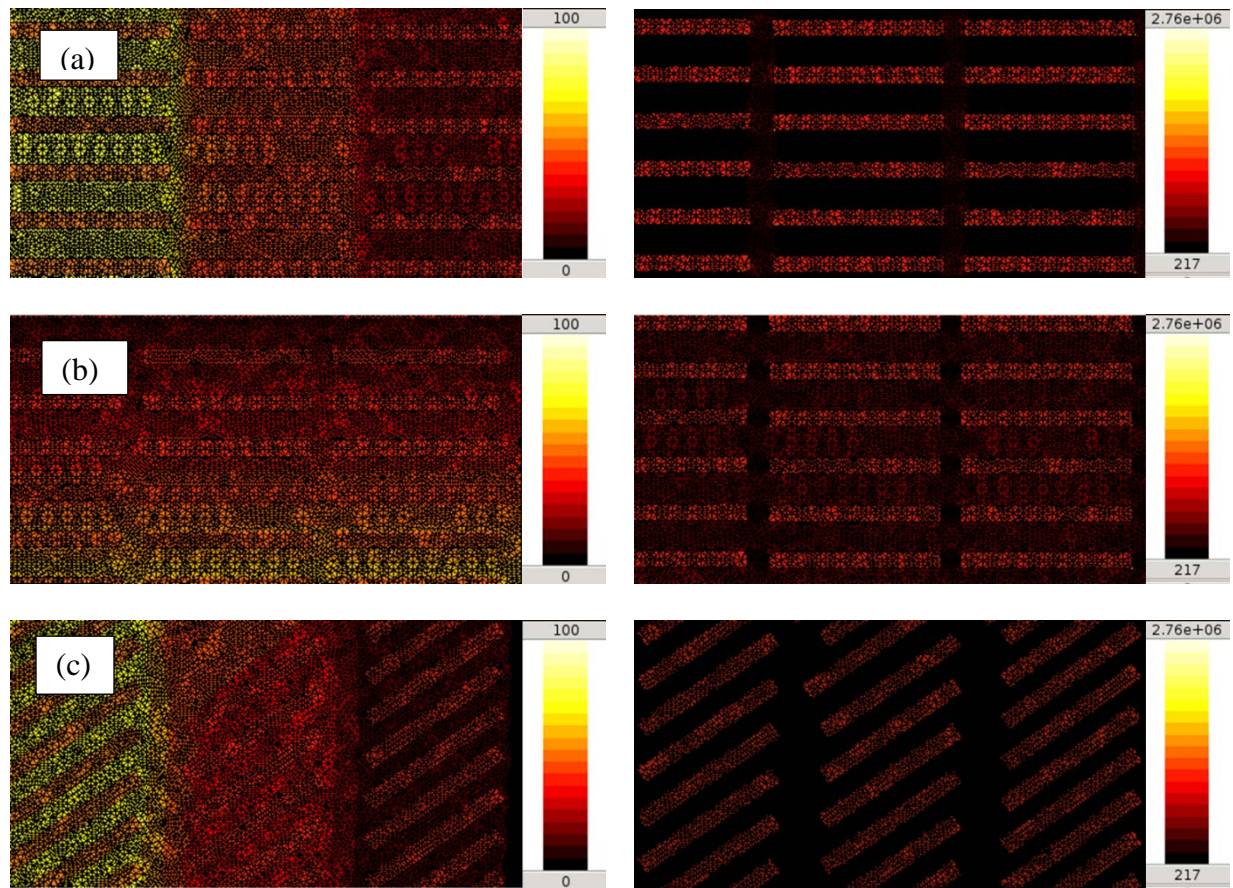


Figure 2-8: Temperature (left) and heat flux (right) contour plot of three different orientations: (a) case-1 (longitudinal), (b) case-2 (perpendicular), and (c) case-1 (angled).

Table 2-2: Predicted thermal conductivity of BN-BMI composites in FEA-1

Sample wt% of BN	Thermal Conductivity (W/m/K)		
	\parallel	T	/
24% BN	0.74	0.23	0.29
43% BN	1.06	0.28	0.42
54% BN	1.18	0.33	0.61
63% BN	1.24	0.42	0.81
72% BN	1.29	0.55	0.98
80% BN	1.32	1.22	1.01

2.4.2 Diameter Effect

Five different samples at 30% weight percentage filler are prepared with different diameters of the filler ranging from $20\mu\text{m}$ – $100\mu\text{m}$ keeping the aspect ratio (D/t) same as 10.

The change of effective thermal conductivity with respect to diameter at a fixed weight % is shown in Figure 2-9. It shows that up to 80 μm diameter there is no significant change in the properties whereas at 100 μm , the conductivity increases suddenly from 0.57 W/m/K to 1.06 W/m/K. All of these samples at different diameters are at a constant volume. The sudden increment at 100 μm may be explained by two factors: surface area of contact and the length of heat conduction through the particles. At lower diameters, the surface area of contact between the resin and particle is more but the length of heat conduction through the conducting particle is less and vice versa for the higher diameter of the particles. These two effects are competitive up to a certain value of diameter and at 100 μm the effect of head conducting path through the particle is dominating and the effective thermal conductivity increases suddenly.

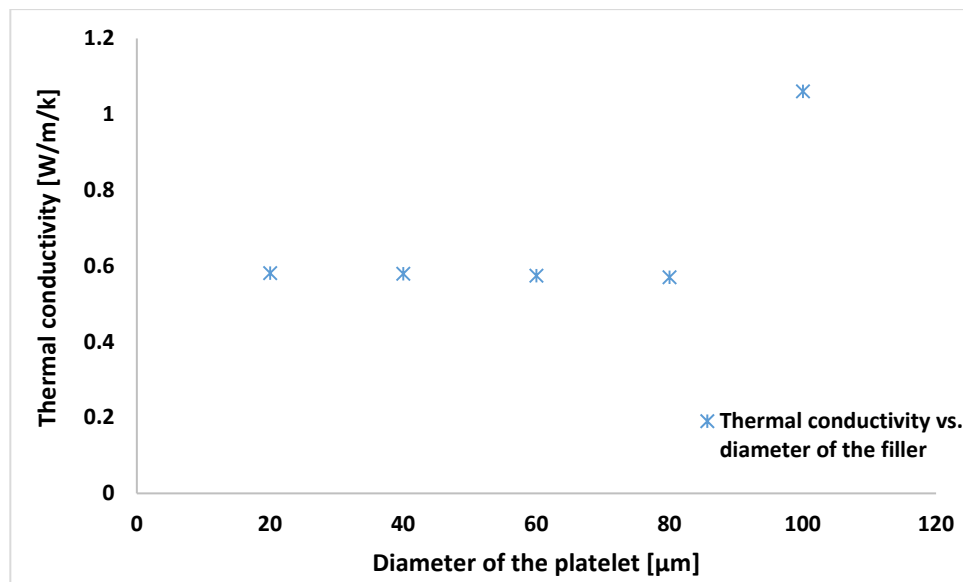


Figure 2-9: Thermal conductivity vs. diameter of the platelet at a fixed aspect ratio and weight %

2.4.3 Effect of Particle Interconnected Network

The preceding prediction considers the particles are interconnected where at higher concentrations the particles got interconnected with each other and form a network. This will be discussed more in next sections (FEA-2). Therefore, to observe the effect of interconnection at

higher concentrations (70% and 80% as observed from the experimental data), we form the network of the particle arbitrarily and predict their properties. Figure 2-10 clearly shows the increase of their properties due to the formation of network at 80% loading of BN platelets.

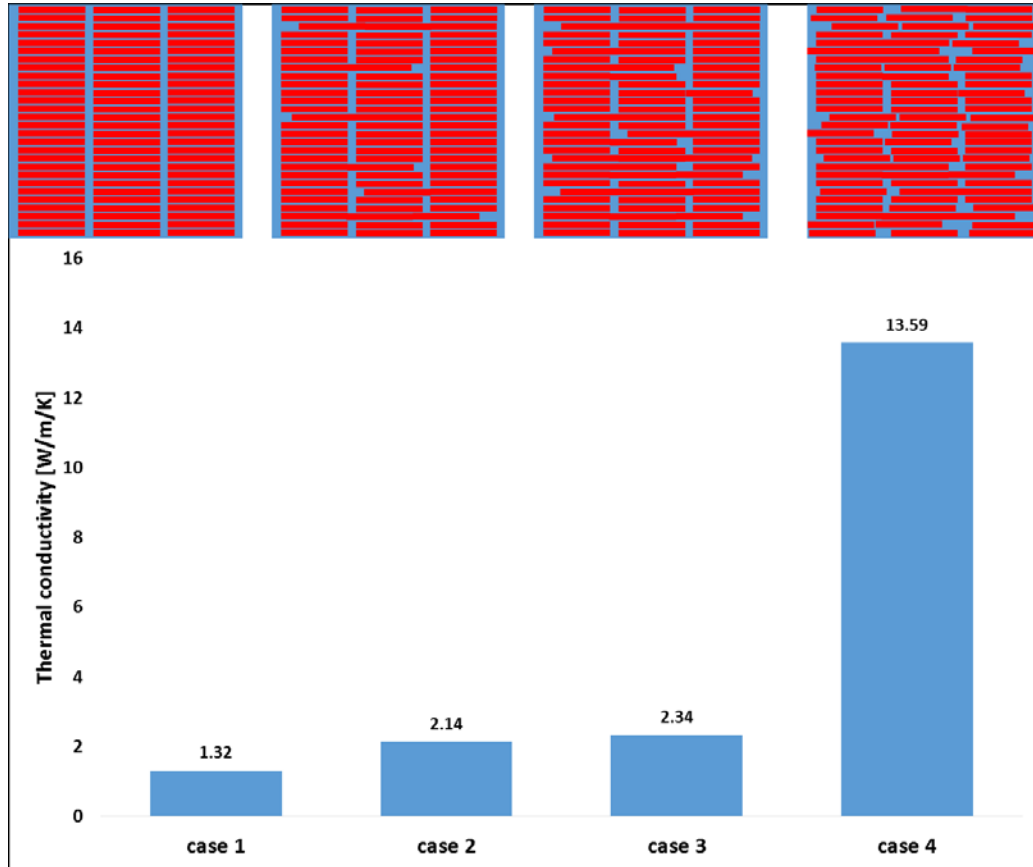


Figure 2-10: The effect of thermal conductivity of particle interconnection (80% BN by wt.).

2.5 Comparison with Experiments

For validation purposes, we use transient heat transfer analysis to measure experimental thermal conductivity for different volume fractions of BN platelets of different diameters. Figure 2-11 shows the comparison between simulation and experimental results.

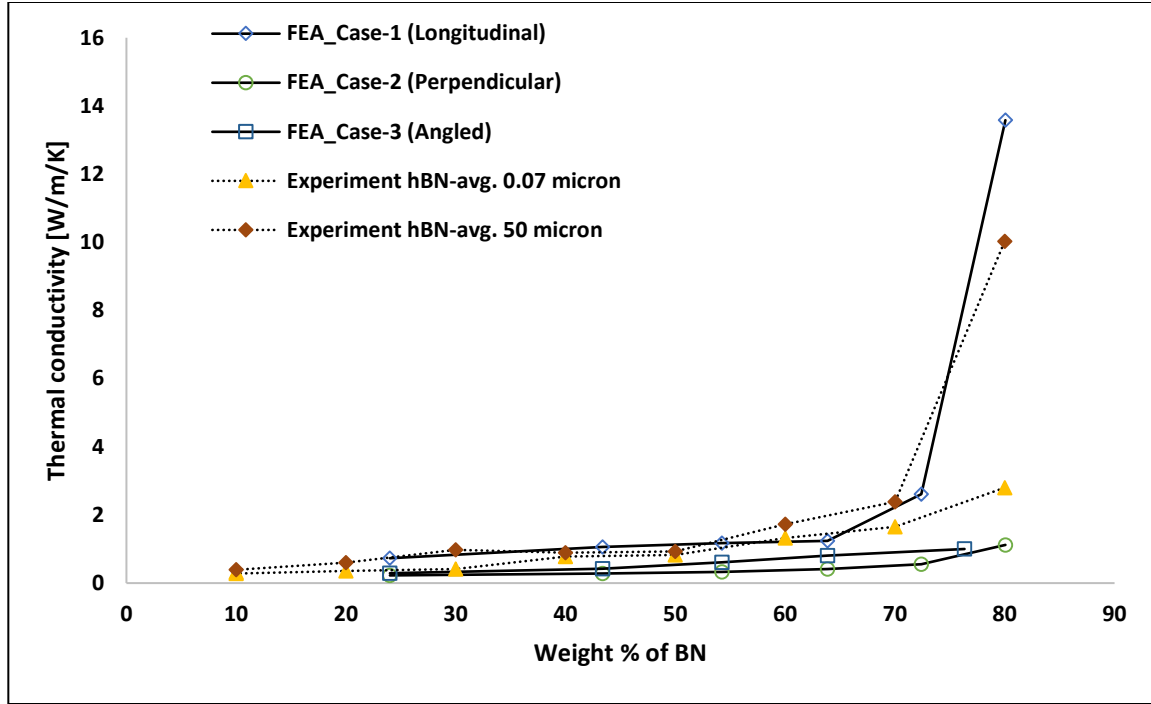


Figure 2-11: Comparison of simulation thermal conductivity with experimental values.

It has been found that there is an excellent agreement between those two results considering the percolations of the platelets at the higher loading fractions (70% and 80% of BN). The effect of percolation has been mentioned in literature [19]. Previously, perfectly homogeneous distribution was considered in all simulations, whereas later on the percolations of the platelets are considered for higher concentrations.

2.6 FEA-2

Scanning electron microscope (SEM) images at two different weight fractions of platelets (20% and 80%) is reported in Figure 2-12, which shows there is percolation at higher weight fractions of BN platelets. The SEM images have been taken from previous study [18]. We are now interested in simulating the thermal behavior on the exact microstructure obtained as SEM images at 20% and 80% weight fraction of BN platelets. OOF2 works in planar condition and therefore

out of plane platelets (as shown in Figure 2-12 for 80%) are removed very carefully while binary images are produced for the simulations. Figure 2-13 shows the meshing and temperature gradient of a portion along with the polished SEM image for simulation at 80% weight percentage.

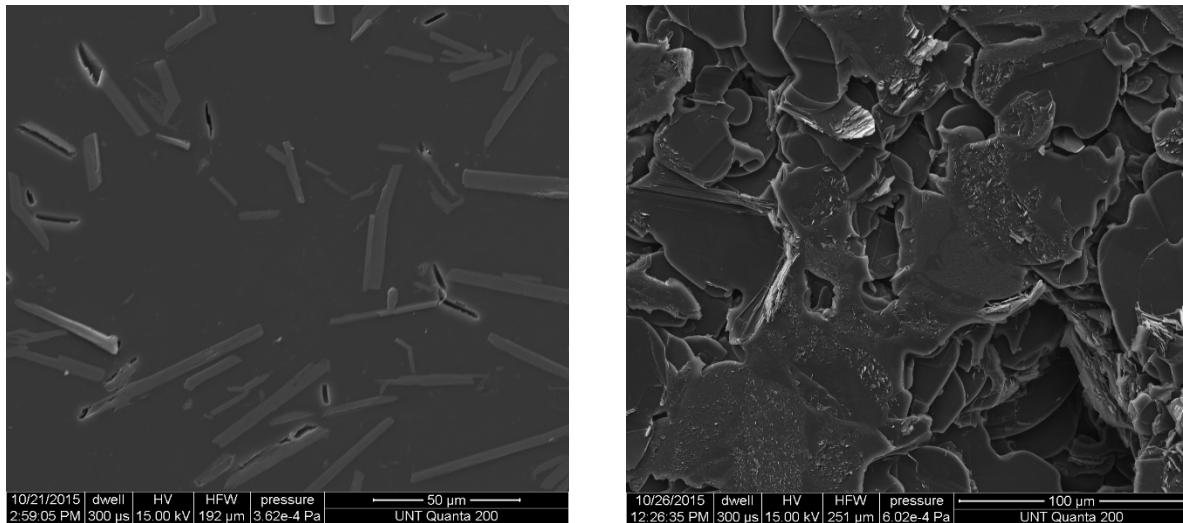


Figure 2-12: SEM images of BN platelet filled BMI: 20% (left) and 80% (right) weight fraction of BN [18].

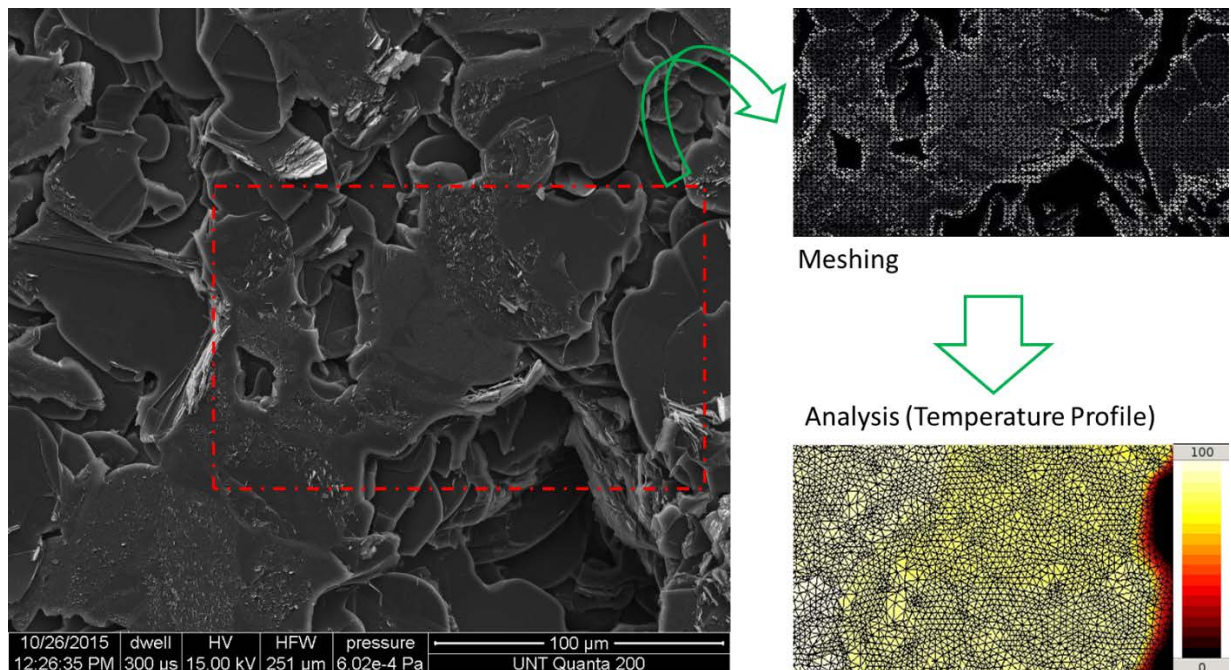


Figure 2-13: Polished SEM image of 80% BN platelets, a portion of the meshed structure and temperature profile.

The direction of heat flow is considered both in the $-x$ and the $-y$ directions for the both SEM microstructures and their averages are taken as the effective thermal conductivities, as shown in Figure 2-14. Simulated thermal conductivities for 80% BN in the $-x$ direction is $K_{eff,x} = 12.27 \frac{W}{mK}$ and in the $-y$ direction is $K_{eff,y} = 11.2 \frac{W}{mK}$; and for 20% BN in the $-x$ direction is $K_{eff,x} = 0.66 \frac{W}{mK}$ and in the $-y$ direction $K_{eff,y} = 0.51 \frac{W}{mK}$. Even though, the particles are randomly distributed, the bulk properties of the composites in $-x$ and $-y$ directions are showing different properties due to the anisotropic properties of the particles. Therefore, the averaged effective thermal conductivities from simulation of 20% and 80% filled BMIs are 0.59 and 11.73 $W/m/K$, whereas experiment determines these two values as 0.6 and 10.3 $W/m/K$. Figure 2-14 shows the comparison between the predicted and experimental results. The simulation result based on the SEM images at 20% filler loading agrees well with the experimental results but the simulation overestimates a little at 80% filler concentration compared to the experimental result. This is because, simulation considers perfect thermal contact with no loss of properties for the whole block of percolated particles. But in actual, the contact region of the percolated platelets should not possess the same thermal conductivity as its isotropic properties because the processing temperature of sample preparation is far below the melting point of the platelets.

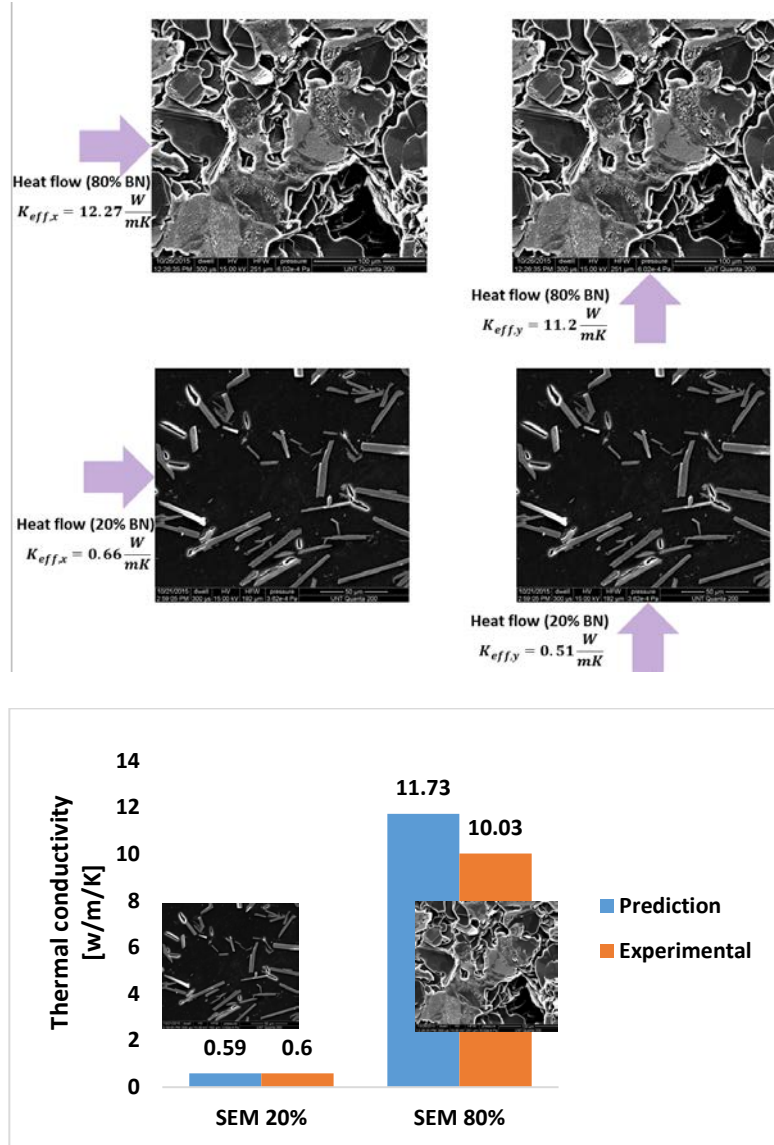


Figure 2-14: Comparison between the predicted and experimental thermal conductivity based on SEM images of 20% and 80%

2.7 Conclusions

Orientation dependent thermal conductivity has been modeled in this study for anisotropic materials property of boron nitride platelet. Due to increasing the filler content, effective thermal conductivity increases significantly. The effect of diameter of the filler is also investigated using this model. Up to a certain diameter, there is no noticeable change in the property and after that,

the conductivity increased sharply due to the fact that the length of heat conduction through the conducting particle becomes more dominant than the surface area of contact between the resin and particles at higher diameters. The comparison between simulation and experiment is performed which shows an excellent agreement. Therefore the conclusions of this study are:

- FEA predicts well at lower concentrations of BN of the modeled microstructure but underestimates at higher concentrations of those without the percolations. Considering the percolations they agree well at both lower and higher concentrations.
- SEM image based FEA predicts well both at lower and higher concentrations.
- The sensitivity of diameter of the platelets are not as strong at lower concentrations as it is at higher concentrations.

2.8 References

- [1] Zweben, C. (1998). Advances in composite materials for thermal management in electronic packaging. *Jom*, 50(6), 47-51.
- [2] Luo, T., & Lloyd, J. R. (2012). Enhancement of thermal energy transport across graphene/graphite and polymer interfaces: a molecular dynamics study. *Advanced Functional Materials*, 22(12), 2495-2502.
- [3] Balandin, A. A. (2011). Thermal properties of graphene and nanostructured carbon materials. *Nature materials*, 10(8), 569-581.
- [4] Marconnet, A. M., Yamamoto, N., Panzer, M. A., Wardle, B. L., & Goodson, K. E. (2011). Thermal conduction in aligned carbon nanotube–polymer nanocomposites with high packing density. *ACS nano*, 5(6), 4818-4825.
- [5] Lin, Z., Liu, Y., Raghavan, S., Moon, K. S., Sitaraman, S. K., & Wong, C. P. (2013). Magnetic alignment of hexagonal boron nitride platelets in polymer matrix: toward high performance anisotropic polymer composites for electronic encapsulation. *ACS applied materials & interfaces*, 5(15), 7633-7640.
- [6] Tanimoto, M., Yamagata, T., Miyata, K., & Ando, S. (2013). Anisotropic thermal diffusivity of hexagonal boron nitride-filled polyimide films: effects of filler particle size, aggregation, orientation, and polymer chain rigidity. *ACS applied materials & interfaces*, 5(10), 4374-4382.

- [7] Terao, T., Zhi, C., Bando, Y., Mitome, M., Tang, C., & Golberg, D. (2010). Alignment of boron nitride nanotubes in polymeric composite films for thermal conductivity improvement. *The Journal of Physical Chemistry C*, 114(10), 4340-4344.
- [8] Coker, Z., Diaz, H., D'Souza, N., & Choi, T. Y. (2014, May). Boron Nitride Nanoparticles-based thermal adhesives for thermal management of high-temperature electronics. In *Thermal and Thermomechanical Phenomena in Electronic Systems (ITherm)*, 2014 IEEE Intersociety Conference on (pp. 421-425). IEEE.
- [9] Zeng, X., Yu, S., & Sun, R. (2013). Thermal behavior and dielectric property analysis of boron nitride-filled bismaleimide-triazine resin composites. *Journal of Applied Polymer Science*, 128(3), 1353-1359.
- [10] Ishida, H., & Rimdusit, S. (1998). Very high thermal conductivity obtained by boron nitride-filled polybenzoxazine. *Thermochimica Acta*, 320(1), 177-186.
- [11] Gao, Y., Gu, A., Jiao, Y., Yang, Y., Liang, G., Hu, J. T., & Yuan, L. (2012). High-performance hexagonal boron nitride/bismaleimide composites with high thermal conductivity, low coefficient of thermal expansion, and low dielectric loss. *Polymers for Advanced Technologies*, 23(5), 919-928.
- [12] <http://www.ctcms.nist.gov/oof/oof2>
- [13] Reid, A. C., Lua, R. C., García, R. E., Coffman, V. R., & Langer, S. A. (2009). Modelling microstructures with OOF2. *International Journal of Materials and Product Technology*, 35(3-4), 361-373.
- [14] Bakshi, S. R., Patel, R. R., & Agarwal, A. (2010). Thermal conductivity of carbon nanotube reinforced aluminum composites: a multi-scale study using object oriented finite element method. *Computational Materials Science*, 50(2), 419-428.
- [15] Chawla, N., Patel, B. V., Koopman, M., Chawla, K. K., Saha, R., Patterson, B. R., & Langer, S. A. (2002). Microstructure-based simulation of thermomechanical behavior of composite materials by object-oriented finite element analysis. *Materials Characterization*, 49(5), 395-407.
- [16] Angle, J. P., Wang, Z., Dames, C., & Mecartney, M. L. (2013). Comparison of Two-Phase Thermal Conductivity Models with Experiments on Dilute Ceramic Composites. *Journal of the American Ceramic Society*, 96(9), 2935-2942.
- [17] Sharma, N. K., Pandit, S. N., & Vaish, R. (2012). Microstructural Modeling of Ni-Composites Using Object-Oriented Finite-Element Method. *ISRN Ceramics*, 2012.
- [18] Warner, Nathaniel, Investigation of the effect of particle size and particle loading on thermal conductivity and dielectric strength of thermoset polymers, MS thesis (Mechanical and Energy Engineering), December 2015, University of North Texas.

[19] Gerhardt, R. A., Runyan, J., Sana, C., McLachlan, D. S., & Ruh, R. (2001). Electrical Properties of Boron Nitride Matrix Composites: III, Observations near the Percolation Threshold in BN-B₄C Composites. *Journal of the American Ceramic Society*, 84(10), 2335-2342.

CHAPTER 3

MOLECULAR DYNAMICS SIMULATIONS FOR THERMAL CONDUCTIVITY

3.1 Introduction

Molecular dynamics (MD) simulations have widely been used for predicting continuum properties and designing materials by considering molecular interaction in atomic level. In order to estimate different kinds of phenomena such as thermal, mechanical, and electrical properties, different types of methods have been developed. In MD simulations, atoms are interacted through atomic potentials such as harmonic/anharmonic constraint and always oscillate with respect to the position of minimum energy. Therefore, an atomic model always seeks to find a configuration of minimum energy state. MD simulations are performed to understand the thermal transport of polymers and their composites with the atomic level phenomena [1-6]. Sun et al. showed the functionalized surface with a self-assembled mono layer (SAM) increases the thermal transport across hard-soft material interface using MD simulations [1]. Teng et al. showed that in polymers with rigid backbone ($\pi - bond$), strong inter-chain interactions suppress the segmental rotation and offer high thermal conductivity [2]. Morphology of a single chain [3], amorphous structure of the bulk polymer [4], plays an important role to control the thermal conductivity. Bulk amorphous polymer has low thermal conductivity than a single chain due to the inter-chain scattering and suppression of acoustic phononic modes. In general, simulations consider perfect microstructure and ideal condition. Therefore, thermal conductivities of bent carbon nanotube instead of straight one (considering defect) [5] and in stretched condition under mechanical loading [6] have been estimated using molecular simulation. The effect of platelet geometry with its orientations and arrangement using MD simulation is not reported yet. In this study, molecular model of pure cross-linked BMI with different concentrations of BN nano-platelets in different orientations are

constructed. All geometries are optimized to find the minimum energy state and analyzed with reverse non-equilibrium molecular dynamics (RNEMD) simulations to predict thermal conductivity.

3.2 Methodology

3.2.1 Constructing Molecular Model

The construction begins with defining a monomer of BMI as shown in the inset of Figure 3-1. Then this structure is replicated to three monomers as a group and then this group is crosslinked to the similar group which makes 6 monomers in total. These monomers are now replicated and crosslinked with each other making the number of monomer as 12. After repeating this steps one more time, we obtain total 24 monomers in a chain. Amorphous module of Materials studio [7] is now used to replicate 10 chains of this structure (24 monomers in a chain) and these chains are crosslinked. The initial configuration holds a density of 0.85 g/cm^3 whereas we found experimental density is 1.12 g/cm^3 . Initial model is prepared with lower density for taking the advantages of easier convergence of the structure. Then the energy is minimized using Discover module. Afterward, the simulation box is compressed to the desired experimental density 1.12 g/cm^3 . This structure is not at the minimum energy state. Therefore, the energy is minimized again with isothermal-isobaric ensemble i.e. NPT ensemble (constant number of atoms, constant pressure and temperature) and run with 0.1 femtosecond (fs) time step for 100 picosecond at 298K temperature and 1 atmosphere pressure. This will minimize the energy of the system as well as collapse/expand the simulation box for maintaining the required pressure and temperature at the same time. By this, we obtain the equilibrium structure of the model. The final density of this pure BMI at atmospheric temperature and pressure is calculated as 1.17 g/cm^3 which is in good

agreement with experimental results. The tetragonal simulation box is used with a dimension as $a = 4.2 \text{ nm}$, $b = 4.2 \text{ nm}$, and $c = 7.2 \text{ nm}$, which is elongated in z-direction. The reason for this elongation in z-direction is to facilitate the heat flow along this direction and reduces the other components for considering a one directional heat flow. Figure 3-1 shows the equilibrium structure of cross-liked BMI. After obtaining the molecular model of pure BMI, we now focus on constructing boron nitride (BN) filled BMI composite. Therefore, a 5×5 boron nitride hexagonal platelet is constructed and this is replicated three times to form a group of four BN platelets. This structure is now optimized to obtain the geometry with lowest energy in FORCITE module. The interlayer gap of the optimized geometry is found as 3.6 angstrom (0.36 nanometer), which is shown in the inset of Figure 3-2. For the layered structure of BN, a boron atom of a layer occupies a position which is exactly on top or bottom of a nitrogen atom of the next layer to it and a nitrogen atom of a layer is on top or bottom of a boron atom of the next layer to it as shown in reference [8]. Now this group of layers is incorporated in pure BMI in multiple numbers in order to construct BN-BMI composite at three different weight fractions. For each weight fraction, the platelets are also placed in three different orientations with respect to z-axis (the measured direction of the thermal conductivity). Figure 3-2 shows the three different orientations of the platelets: longitudinal, perpendicular, and angled with respect to z-axis for the BN-BMI composite of 56% BN platelet (by weight percentage). All geometries are then optimized using FORCITE module of the software, as this module will be used to calculate the thermal conductivity applying RNEMD, which will be discussed in next sections.

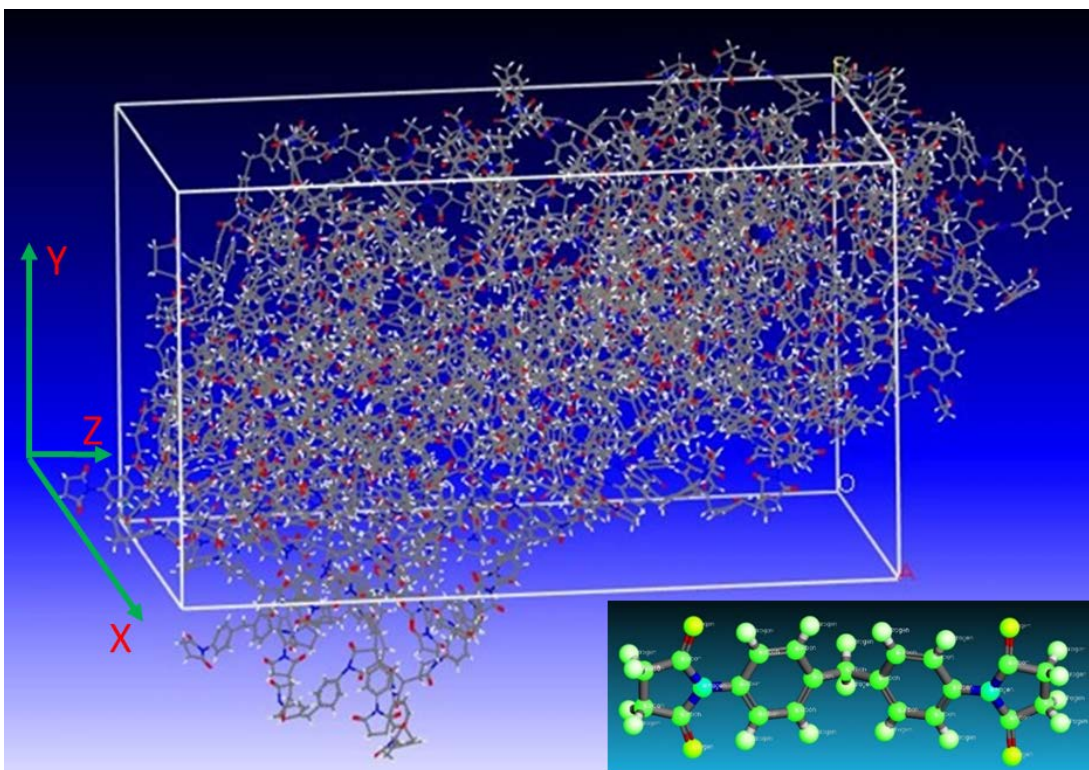


Figure 3-1: Molecular structure of cross-liked BMI (monomer is in the inset)

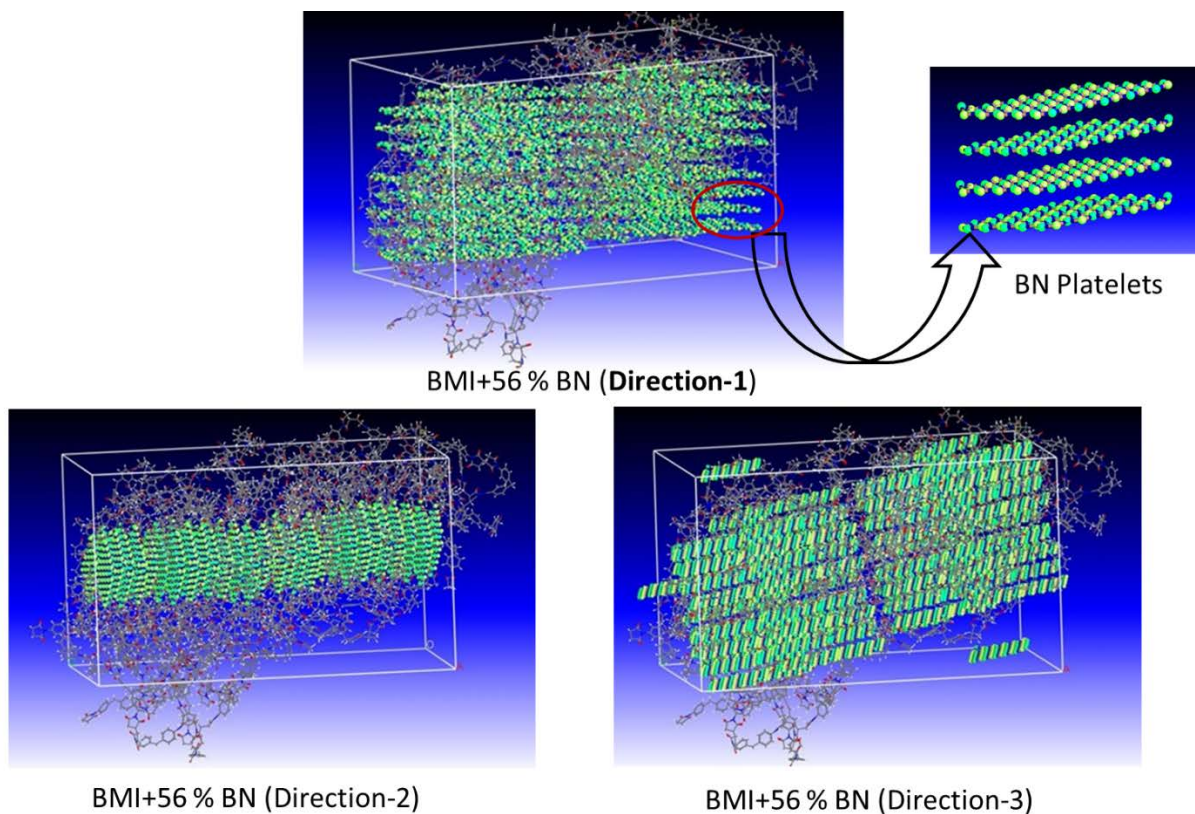


Figure 3-2: Three different orientations of the BN platelets of BN-BMI composite at 57% weight percentage of BN.

3.2.2 Reverse Non-Equilibrium Molecular Dynamics (RNEMD) Simulation

Thermal conductivity is measured as the ratio of heat flux in the direction of heat flow and the temperature gradient in that direction. Equilibrium molecular dynamics simulation is a natural simulation experiments, where a temperature gradient is imposed and the generated heat flux is calculated [9-10]. But the limitation of that equilibrium MD are: (1) heat flux converges very slowly and (2) large temperature gradient is necessary to create noticeable flux out of noise. In non-equilibrium MD, the reverse action is performed, where heat flux is imposed and temperature gradient is measured over time. In a sense it is called reverse because it is reverse cause and action compared to experiment or conventional MD simulation [11]. As the method reported, for

imposing the flux and measuring resultant temperature gradient, the whole simulation box is divided into N slabs with identical thickness. Temperatures of the slabs are calculated from the velocities of the molecules in those slabs using statistical mechanical principle, where temperature of a system is related to the kinetic energy of the particles. The heat flux is generated by exchanging velocity vectors between the hottest atom in the cool slab and the coolest atom in the hot slab. This initial method is first developed for monoatomic fluids, later on for materials with holonomic constraints exchanging the center of mass velocity is suggested by Bedrov et al. [10]. In both cases, conservation of energy is satisfied i.e. the total kinetic energy and linear momentum is kept unchanged. For multicomponent system with heterogeneous masses, particle with highest kinetic energy is considered instead of the faster molecule in cold region and vice versa for the hot region [12]. This considers the energy and momentum exchange between cold and hot slabs, where it keeps the total energy and momentum constants for the system [12]. At each time interval (Δt), two fixed layers exchange an energy ΔE to generate the flux, where the flux would be:

$$J = \frac{1}{2A} \frac{\Delta E}{\Delta t} \quad (3-1)$$

where, A is the cross-sectional area of heat flow, the factor 2 is due to periodic boundary conditions. The calculated thermal conductivity is dependent on the degree of freedom of the model, and therefore different force-fields have been tested for amorphous polyamide-6,6 [13]. There are several control parameters of the simulation for the calculation of flux and resultant temperature gradient such as: the interval or number of time step between velocity exchanges, the exchange method of constant temperature or constant energy, simulation length, and degrees of freedom [9-11, 13] but it has been concluded that the calculated thermal conductivities are relatively insensitive to the variations in the RNEMD parameters [11]. The purpose of this study is rather test the capacity of the developed method for designing high thermal conductive BMI-

BN composites based on orientations, loading fractions, and interconnections. All of the models, as constructed in last section, are subdivided with 40 layers and run using Universal force field [14]. Brendensen thermostat is used with a decay constant of 0.1. The number of exchanges is taken as 1000 during the calculation stage. The results are found to be converged after 10 picoseconds (ps) running with a 0.1 femtosecond (fs) time step. All simulations are performed at room temperature 298K.

3.3 Results

At first, the thermal conductivity of pure BMI is measured. The temperature gradient along the Z –direction are shown in Figure 3-3.

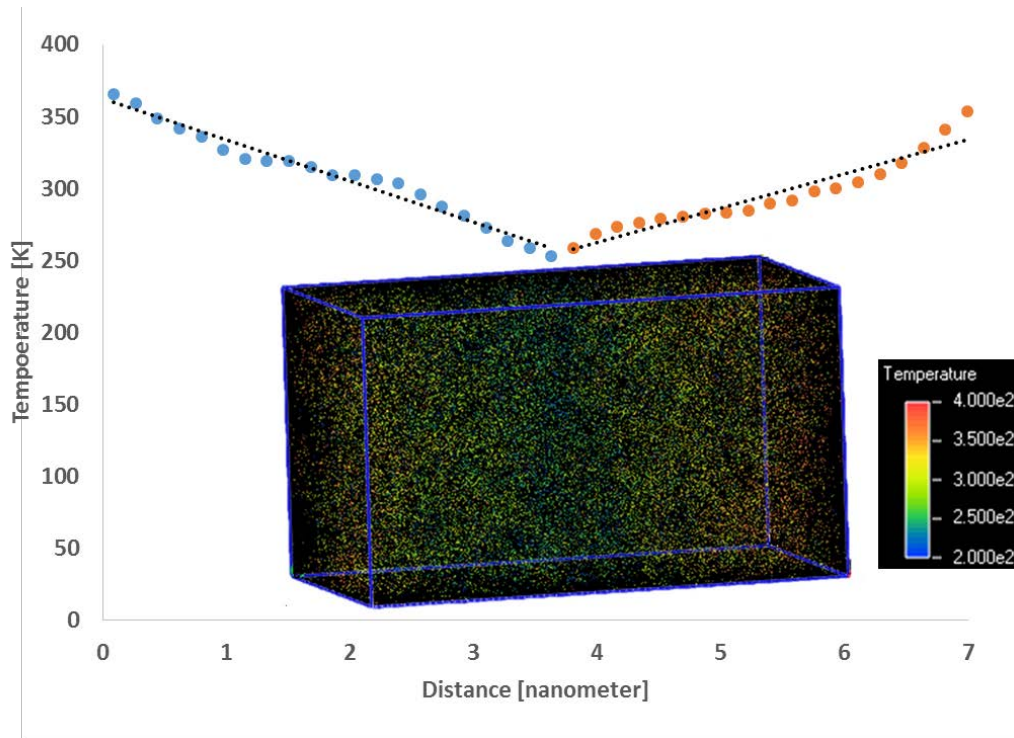


Figure 3-3: Contour plot of temperature gradient of the simulation box (left), temperature gradient along Z-direction (right)

The measured thermal conductivity of BMI is found as $0.2 \frac{W}{mK}$ which is in excellent agreement with the experimental value of BMI as $0.19 \frac{W}{mK}$. Therefore, we now measure thermal conductivity of BN filled BMI at three different orientations for different weight fractions of the filler. Figures 3-4 to 3-6 show the orientation dependent thermal conductivities for the weight fractions of 39%, 56%, and 80%, respectively. The predicted thermal conductivity from the molecular dynamics simulations are compared with experimental results (obtained from previous study [15]) in Figure 3-7, where both results are in excellent agreement.

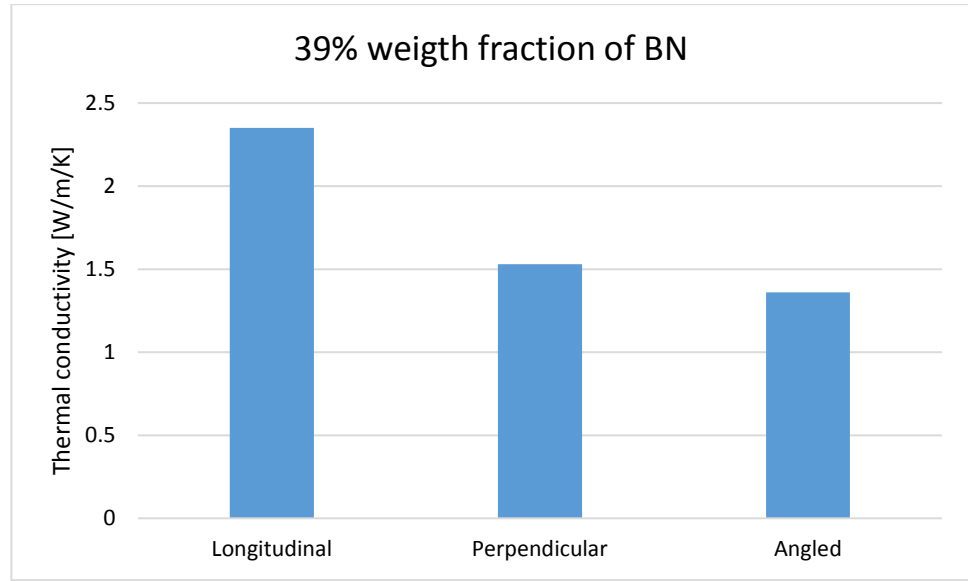


Figure 3-4: Thermal conductivity at three different orientations at 39% weight fraction of BN platelets

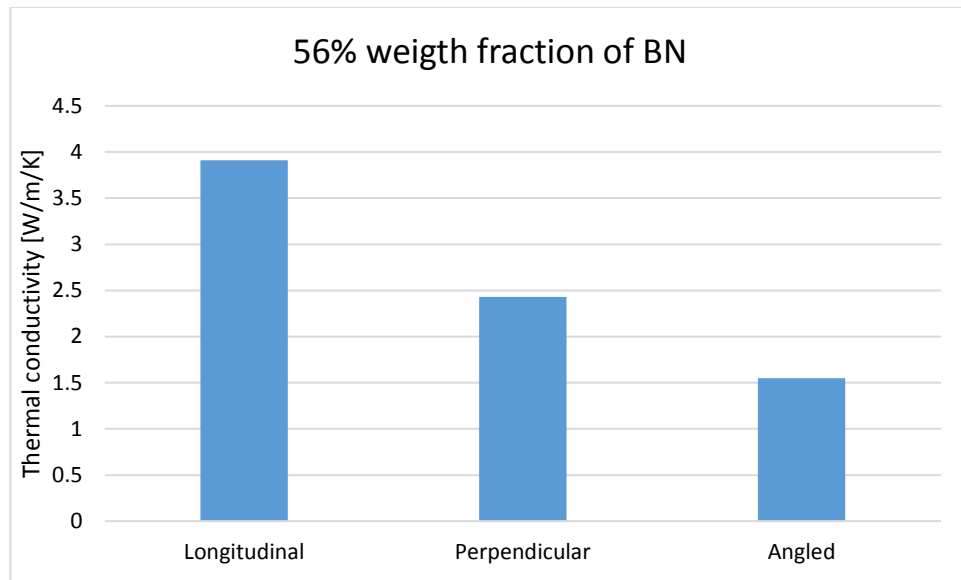


Figure 3-5: Thermal conductivity at three different orientations at 56% weight fraction of BN platelets

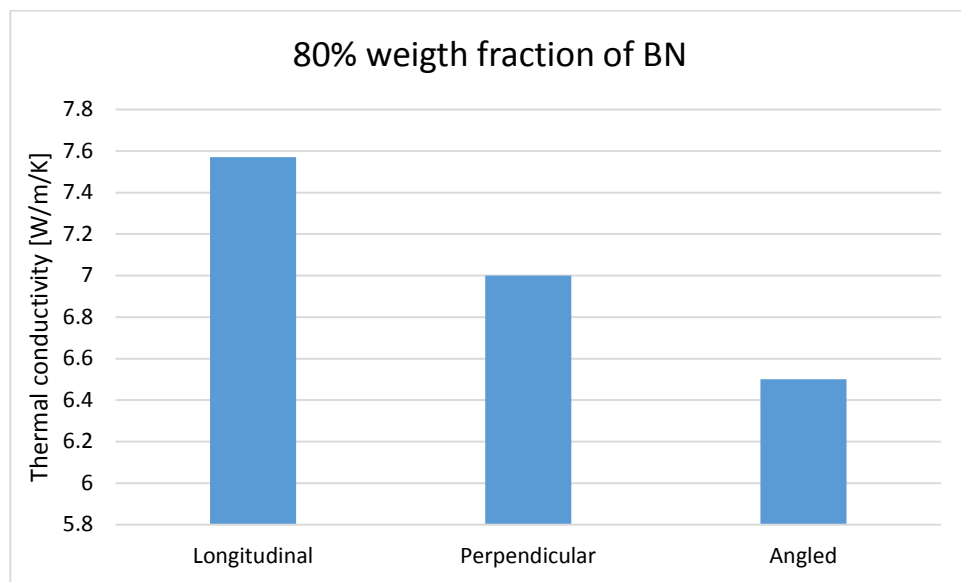


Figure 3-6: Thermal conductivity at three different orientations at 80% weight fraction of BN platelets

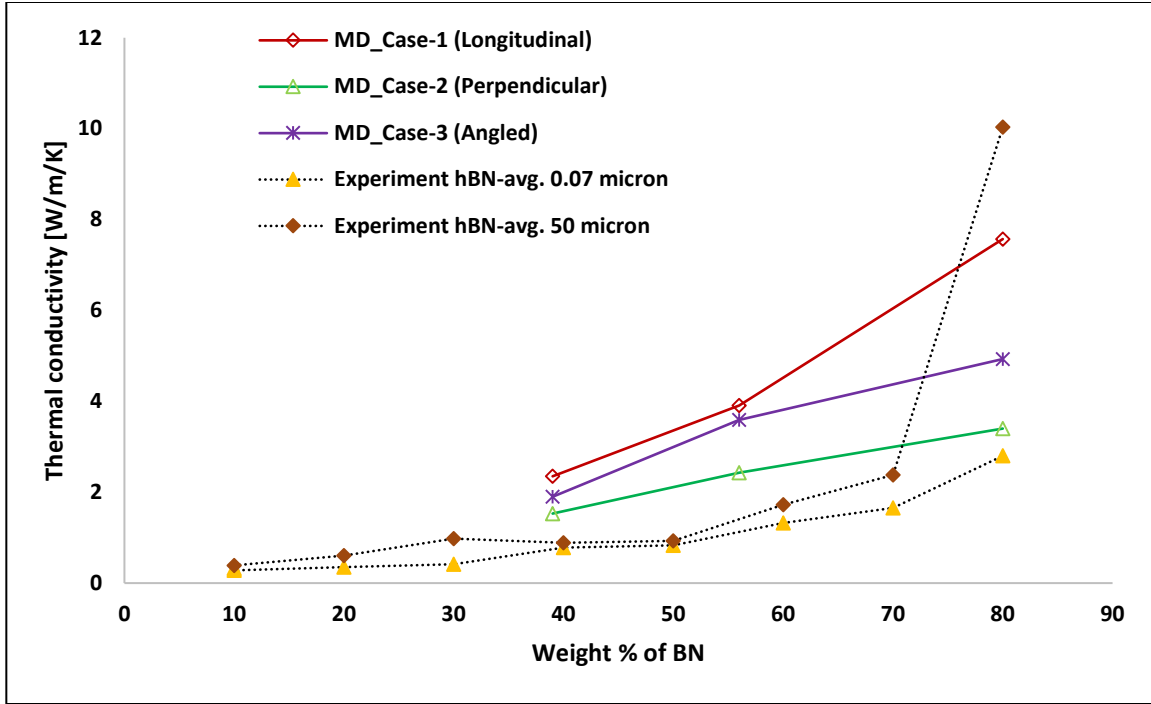


Figure 3-7: Comparison of predicted results from molecular dynamics simulations with the experimental measurements

3.4 Conclusions

Molecular dynamics simulations have been performed in this study to measure thermal conductivity by considering molecular interactions. Crosslinked BMI model is prepared with experimental density with a tetragonal simulation box, extended in Z –direction (the direction of measuring the thermal conductivity). Boron nitride platelets are constructed and the geometry is optimized. Afterward, BN platelets are incorporated in the pure BMI model at three different weight fractions in three different orientations. All models are equilibrated and optimized prior to measuring the thermal conductivity. Non-equilibrium molecular dynamics simulations are performed to impose the energy flux and measure the thermal gradient. The ratio of these two terms give the measure of thermal conductivity. From simulations, it is clearly evident that the

alignment of the BN platelets have an impact on bulk thermal conductivity. It is also found that by increasing the weight percentage of BN platelets, thermal conductivity of BMI increases conspicuously. Therefore, this study shows a clear guidance to the design of composite materials with filler reinforced in order to maximize the thermal transport.

3.5 References

1. Sun, F., Zhang, T., Jobbins, M. M., Guo, Z., Zhang, X., Zheng, Z., & Luo, T. (2014). Molecular Bridge Enables Anomalous Enhancement in Thermal Transport across Hard-Soft Material Interfaces. *Advanced Materials*, 26(35), 6093-6099.
2. Zhang, T., Wu, X., & Luo, T. (2014). Polymer Nanofibers with Outstanding Thermal Conductivity and Thermal Stability: Fundamental Linkage between Molecular Characteristics and Macroscopic Thermal Properties. *The Journal of Physical Chemistry C*, 118(36), 21148-21159.
3. Zhang, T., & Luo, T. (2012). Morphology-influenced thermal conductivity of polyethylene single chains and crystalline fibers. *Journal of Applied Physics*, 112(9), 094304.
4. Luo, T., Esfarjani, K., Shiomi, J., Henry, A., & Chen, G. (2011). Molecular dynamics simulation of thermal energy transport in polydimethylsiloxane. *Journal of Applied Physics*, 109(7), 074321.
5. Huang, Z., Tang, Z. A., Yu, J., & Bai, S. (2011). Temperature-dependent thermal conductivity of bent carbon nanotubes by molecular dynamics simulation. *Journal of Applied Physics*, 109(10), 104316.
6. Cho, M., Yu, S., & Yang, S. (2011). Thermal transport properties of nanoparticulate composites under mechanical loading. In *52nd AIAA/ASME/ASCE/AHS/ASC Structures, Structural Dynamics and Materials Conference 19th AIAA/ASME/AHS Adaptive Structures Conference 13t* (p. 1803).
7. Accelrys Software Inc., Sandiego. Available at: <http://accelrys.com/products/materials-studio>.
8. Naftaly, M., Leist, J., & Fletcher, J. R. (2013). Optical properties and structure of pyrolytic boron nitride for THz applications. *Optical Materials Express*, 3(2), 260-269.
9. Müller-Plathe, F., "A simple nonequilibrium molecular dynamics method for calculating the thermal conductivity.", *J. Chem. Phys.*, 106, 6082-6085 (1997).
10. Bedrov, D.; Smith, G.D., "Thermal conductivity of molecular fluids from molecular dynamics simulations: Application of a new imposed-flux method.", *J. Chem. Phys.*, 113, 8080-808 (2000).

11. Zhang, M.; Lussetti, E.; de Souza, L. E. S.; Müller-Plathe, F., "Thermal conductivities of molecular liquids by reverse nonequilibrium molecular dynamics.", *J. Phys. Chem. B*, 109, 15060-15067 (2005).
12. Nieto-Draghi, C.; Bonet Avalos, J., "Non-equilibrium momentum exchange algorithm for molecular dynamics simulation of heat flow in multicomponent systems.", *Mol. Phys.*, 101, 2303-2307 (2003).
13. Lussetti, E.; Terao, T.; Müller-Plathe, F., "Nonequilibrium molecular dynamics calculation of the thermal conductivity of amorphous polyamide-6,6.", *J. Phys. Chem. B*, 111, 11516-11523 (2007).
14. Rappé, A. K., Casewit, C. J., Colwell, K. S., Goddard Iii, W. A., & Skiff, W. M. (1992). UFF, a full periodic table force field for molecular mechanics and molecular dynamics simulations. *Journal of the American chemical society*, 114(25), 10024-10035.
15. Warner, Nathaniel, Investigation of the effect of particle size and particle loading on thermal conductivity and dielectric strength of thermoset polymers, MS thesis (Mechanical and Energy Engineering), December 2015, University of North Texas.

CHAPTER 4

CONCLUSIONS

Anisotropic boron nitride reinforced bismaleimide composites have shown excellent thermal transport as found in this study as well dielectric strength as observed in the previous study [1]. BN has an anisotropic thermal conductivity of 600 W/m/K in the plane and 33 W/m/K through the thickness [2]. Figures 4-1 (a) to (c) show that the alignment of the platelets in planar direction maximize the heat transfer of the composites compared to the out-of-plane direction. The increment of the diameter of the platelets are not very sensitive at low concentrations but they are in high concentrations as shown in Figures 4-1 (a) to (c). Finite element analysis is performed on two types of microstructures: modeled microstructures and SEM images microstructures, whereas modeled microstructures require considering the percolation of the particles at higher concentration. Experiments are performed with transient thermal analysis using a resistance temperature detector (RTD) sensor which acts both as a heater and sensor. FEA results are compared with the experimental results in Figure 4-1(a), which shows good agreement. The FEA based on modeled microstructure without considering percolation underestimates the properties at higher concentrations due to the lack of knowledge about defining percolation, but they agree well at the lower concentrations. The FEA based on SEM image agree well at the lower concentrations but little overestimate at higher concentration due to the drop of properties at the interphase of the particle network at experimental sample but in FEA, perfect contact is assumed.

Reverse non-equilibrium molecular dynamics simulations are performed on molecular models by applying heat flux and measuring the temperature gradient at different locations. The measured thermal conductivities from MD simulations are compared with the experimental

results in Figure 4-1 (b). The MD simulations results are overestimating the properties as perfect molecular structure are considered for simulations but in experimental samples, there are voids and defects. But they are showing the similar trend as shown in experiments.

Therefore, combining all results from different approaches such as experiment, FEA, and MD simulations, they are compared in Figure 4-1 (c), which clearly shows the similar trend of increasing the properties with respect to alignment of the particle as well as the loading fractions.

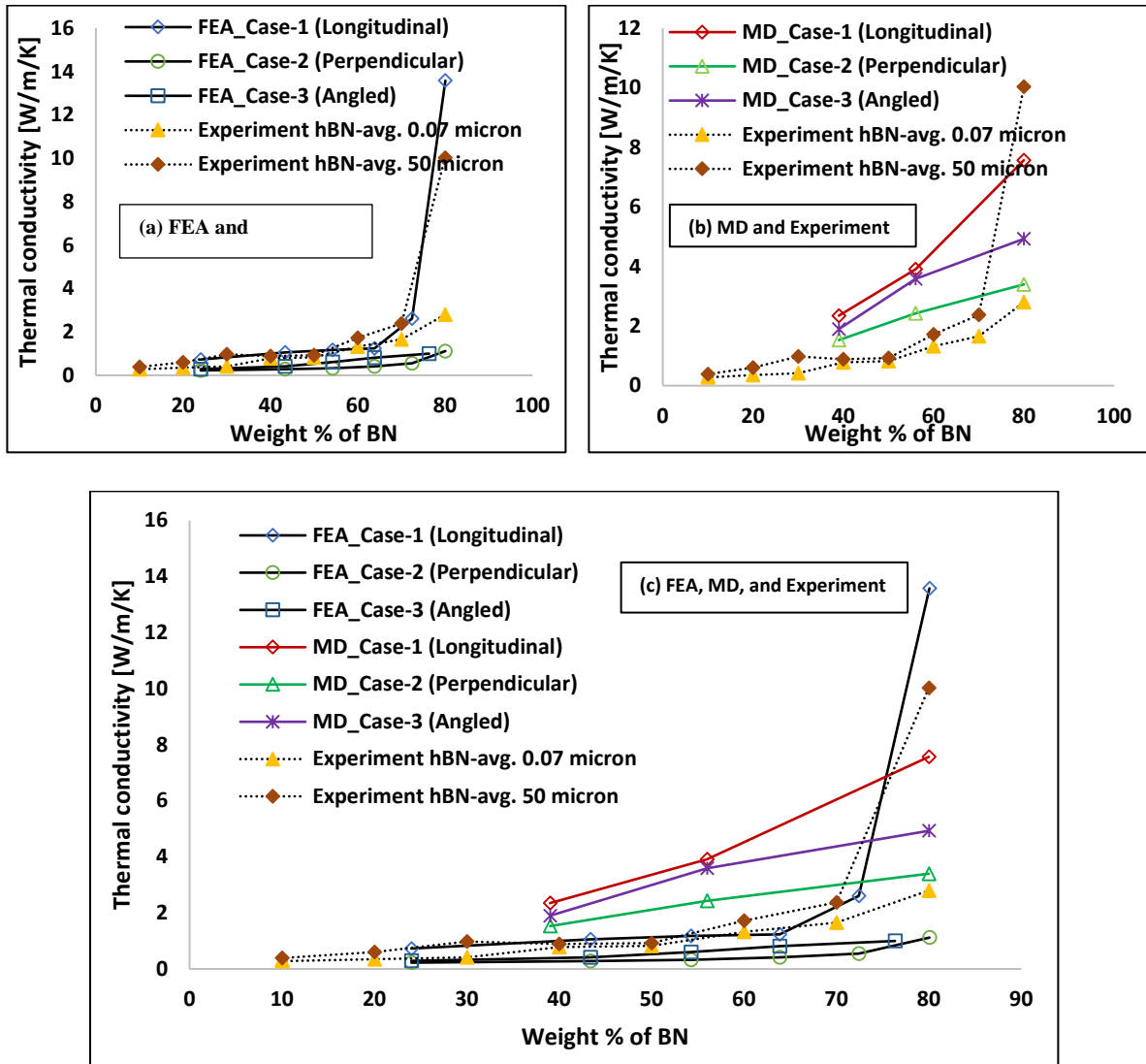


Figure 4-1: (a) Comparison of FEA with experiments, (b) comparison of MD simulations with experiment, and (c) comparison of FEA, MD simulations, and experiment.

4.1 References

[1] Warner, Nathaniel, Investigation of the effect of particle size and particle loading on thermal conductivity and dielectric strength of thermoset polymers, MS thesis (Mechanical and Energy Engineering), December 2015, University of North Texas.

[2] Lin, Z., Liu, Y., Raghavan, S., Moon, K. S., Sitaraman, S. K., & Wong, C. P. (2013). Magnetic alignment of hexagonal boron nitride platelets in polymer matrix: toward high performance anisotropic polymer composites for electronic encapsulation. *ACS applied materials & interfaces*, 5(15), 7633-7640.